Flexural performance of FDM-fabricated PLA composites reinforced with short carbon fiber

R Keshavamurthy
Department of Automotive Technology, Christ University, Bangalore - 560074, India
Keshavamurthy.r@gmail.com, http://orcid.org/0000-0002-8478-0934

Raghu Yogaraju
Department of Mechanical Engineering, B. M. S College of Engineering, Bengaluru-560004, India
Raghuyogaraj.mech@bmsce.ac.in, http://orcid.org/0000-0003-1129-5919

G S Pradeep Kumar
Department of Automotive Technology, Christ University, Bangalore - 560074, India
Pradeepgs.87@gmail.com, http://orcid.org/0000-0003-1737-5549

Mallikarjun Biradar
Department of Mechanical Engineering, Dayananda Sagar Academy of Technology and Management, Bangalore - 560082, India
Mallikarjun-me@dsatm.edu.in, http://orcid.org/0009-0000-1251-1164

Pavan kumar B K
Department of Mechanical Engineering, Ballari Institute of Technology and Management, Ballari-583104, India
Pk22586@gmail.com , http://orcid.org/0000-0003-1295-5712

S Mohan Kumar
Department of Mechanical Engineering, Amrita School of Engineering, Amrita Vishwa Vidyapeetham, Bengaluru-560035, India
S_mohankumar@blr.amrita.edu , http://orcid.org/0000-0001-9317-4410

Shijo Thomas
Department of Automotive Technology, Christ University, Bangalore - 560074, India
shijo.thomas3@gmail.com http://orcid.org/0000-0002-9325-3925

ABSTRACT. Adding short carbon fiber reinforcement to thermoplastic matrices can improve the mechanical performance of additively manufactured polymer-based composites. This work examines the flexural behavior of Fused Deposition Modeling (FDM)-produced polylactic acid (PLA)-based

OPEN ACCESS

Citation: Keshavamurthy, R., Yogaraju, R., Kumar, G. S. P., Biridar, M., Pavan kumar, B. K., Mohan Kumar, S., Thomas, S., Flexural performance of FDM-fabricated PLA composites reinforced with short carbon fiber, Fracture and Structural Integrity, 77 (2026) 217-229.

Received: 04.02.2026
Accepted: 11.04.2026
Published: 03.05.2026
Issue: 07.2026

composites enhanced by short carbon fibers at 3 wt% and 6 wt%. For comparison, unreinforced PLA specimens were also fabricated under identical processing conditions. All the samples were tested for flexural strength using a three-point bend test, following the ASTM standards for polymer composites. The results showed a clear improvement in strength as the reinforcement content increased. The PLA composite with the 3% short carbon fiber reinforcement showed a noticeable increase in load-bearing ability, while the 6% reinforced composite had an impressive 88% higher flexural strength than the plain PLA. To examine how the materials failed, SEM has been utilized to assess the samples' fractured surfaces.

KEYWORDS. Fused Deposition Modelling, Short Carbon Fiber, PLA Composites, Flexural Strength, Fracture Mechanisms.

INTRODUCTION

Additive manufacturing has reshaped the way engineers think about fabrication and honestly it has done so rather quietly [1]. The ability to build intricate geometries while generating comparatively little waste is not something conventional subtractive processes can easily replicate. Among the many techniques that fall under this broad umbrella FDM stands out as the most accessible and economically practical option for producing thermoplastic parts where dimensional accuracy genuinely matters [2]. Industries ranging from food processing to fashion and general manufacturing have adopted this method to construct components that would otherwise demand considerably more effort and expense [3]. As the demand for structurally capable printed parts has grown researchers have turned their attention toward composite filaments and fiber reinforcements in particular with carbon fibers [4] and glass fibers [5] receiving substantial investigative attention over the past decade or so.

Fiber reinforcement is not a new idea. Engineers have been blending fibers into polymer matrices for decades and the mechanical gains are well documented across the literature. Carbon fibers bring an impressive combination of stiffness and low mass and this has made them essentially indispensable in sectors where performance cannot be compromised [6]. Glass fibers are cheaper and still deliver reasonable mechanical performance alongside useful electrical insulation properties though they cannot match carbon fibers in terms of stiffness. Natural fibers sit at the other end of the spectrum offering environmental advantages and moderate strength gains and they degrade over time which is sometimes exactly what a designer wants [5]. Still when the application demands genuine structural performance carbon fiber is generally the reinforcement that gets selected and that preference is well justified [6].

PLA is in many respects the default material for FDM and its widespread use owes a great deal to how easy it is to process as well as its biodegradable character and its relatively low cost. The problem is that neat PLA is not particularly stiff or strong and its thermal resistance leaves something to be desired which limits where it can realistically be deployed [7]. Short carbon fibers change this picture meaningfully by acting on the material at the microstructural level and the improvements in rigidity hardness and thermal stability that result are well supported in the published literature. The processability of PLA is not meaningfully disrupted by the addition of fibers which is practically important when considering FDM as the fabrication route.

Sanei and Popescu [8] produced what is arguably one of the more thorough reviews of 3D printed carbon fiber composites examining how parameters such as nozzle temperature bed temperature infill density infill pattern layer thickness nozzle speed and build orientation each contribute to the final mechanical outcome. Both chopped and continuous fiber configurations were covered and the review conveys a reasonably complete picture of where the field currently stands and where its difficulties lie. Dickson et al. [9] showed that integrating fibers into polymer matrices through Fused Filament Fabrication yields substantial improvements in mechanical performance and the work spans both continuous and short fiber composites across several application contexts. Pervaiz et al. [10] took a somewhat broader view and their assessment covers the processing difficulties inherent to fiber reinforced polymer systems alongside a measured discussion of future possibilities for carbon fiber and high performance polymer blends. Yang et al. [11] focused specifically on continuous fiber thermoplastic composites made via FDM and their analysis of how fiber content printing temperature layer geometry print velocity and layer thickness influence mechanical properties is fairly detailed. Marabello et al. [12] examined the mechanics

of integrating carbon fiber continuously into a polymer matrix and the work connects process decisions to the performance characteristics of the resulting lightweight components.

Maqsood and Rimašauskas [2] looked at how continuous and short carbon fibers affect PLA when the whole system is produced through FDM and their results showed that all reinforced variants outperformed neat PLA in terms of strength and stiffness. Microscopic examination of the printed specimens revealed information about fiber cross linking behavior and helped connect what is happening at the microstructural level to the mechanical response observed during testing.

Most of the studies above relied on commercially available PLA carbon fiber filaments and this is worth pausing on for a moment. Commercial filaments are typically proprietary and the fiber content fiber dimensions and processing histories are rarely disclosed in any meaningful way. This makes it genuinely difficult to isolate the effect of fiber content on mechanical response because the material itself is not fully characterized. The present study takes a different approach by fabricating composite filaments in house using a twin screw extruder at controlled weight fractions of 3 wt% and 6 wt% with short carbon fibers that have been properly characterized. Complete traceability of composition and processing conditions is therefore maintained throughout and the comparison between neat PLA and the two reinforced variants is conducted under identical FDM processing parameters which is arguably the only way to draw conclusions that are genuinely defensible.

The flexural behavior of short carbon fiber-reinforced PLA composites is perhaps less well studied than their tensile behavior, and this represents a real gap in the literature given how commonly structural components encounter bending loads in service. The effect of carbon fiber reinforcement on the flexural strength, flexural modulus, and strain at failure needs to be understood more clearly before FDM-printed PLA can be confidently recommended for demanding structural contexts in automotive and aerospace environments. The objectives of this study are therefore to fabricate PLA carbon fiber composite filaments at 3 wt% and 6 wt% through twin screw extrusion, to print specimens under identical FDM conditions across all material variants, to characterize flexural performance through three-point bend testing in accordance with ASTM D790, and to correlate microstructural observations from fractographic analysis with the macroscopic mechanical data. The results are intended to give engineers and researchers a rigorous and traceable dataset that supports rational material selection and component design wherever bending performance is a critical design driver.

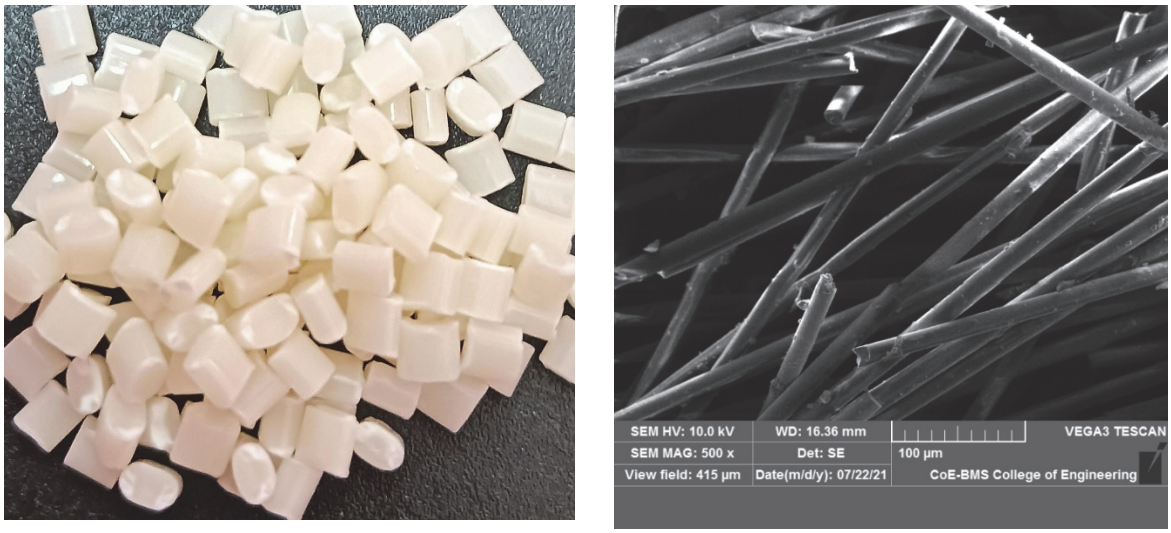

(a) Photograph of PLA Pellets (b) SEM of Short carbon fiber

Figure 1: (a-b) Photograph of PLA pellets and SEM image of short carbon fiber

EXPERIMENTAL DETAILS

Materials and filament extrusion

The material was strengthened using short carbon fibers provided by Tespo international private limited and polymers provided by GLS Polymers in Bangalore, India, as the base material. The short carbon fibers had an average diameter of around 10 microns and lengths of 3 to 5 millimeters. They were elongated and uneven in shape. The PLA pellets were granular in appearance. To assess the effects of these carbon fibers on the composite's bending strengths, the carbon fibers were incorporated into the PLA matrix in two weight percentages, which are 3% and 6%. The composite was

produced via a twin-screw extruder with the purpose of uniformly distributing the carbon fibers within the PLA, after which the composite was in turn pelletized. The composite filament in the pelletized state was used in the FDM technique to produce the test specimens. Samples of PLA without the carbon fibers were also produced for the purpose of comparison in the assessment of the results. After obtaining the neat PLA and composite filaments, they were dried in a vacuum oven for 4 hours at 60°C in order to eliminate all possible moisture present in them, which is fundamental in preventing any hydrolytic breakdown of the filament materials, especially PLA, which is known to change properties significantly in the presence of moisture. Prior drying of the filaments is fundamental in preventing defects such as warping and wettability issues in FDM, which arise as a result of moisture content in the filament material, especially considering the hygroscopic nature of PLA. [13]. PLA pellets and a SEM picture of short carbon fiber are shown in Fig. 1(a-b). Several trials were carried out for different lengths of the filaments, and their details were carefully noted down. The machine had a fixed tolerance of 0.1 mm. When the short carbon fiber mixture incorporated into the polylactic acid filament was examined under standard temperature and pressure conditions, the diameter of the mixture remained constant, and there were no fibers protruding from the matrix. The material had a similar surface to PLA which is confirmed by the Macro inspection.

PARAMETER	3 WT%CF/PLA	6 WT%CF/PLA
Fiber content (weight fraction)	3 WT%	6 WT%
PLA matrix density (g/cm³)	1.24	1.24
Carbon fiber density (g/cm³)	1.76	1.76
Gross fiber volume fraction, (V_f) (vol%) (without infill density correction)	2.15 VOL%	4.35 VOL%
FDM infill density (%)	90%	90%
Effective (net) fiber volume fraction (with infill density correction)	1.9 VOL%	3.9 VOL%

Table 1: Calculated fiber volume fractions for carbon fiber reinforced composites.

FDM PART FABRICATION AND FLEXURAL TEST

The method chosen for the test specimen production is Fused Deposition Modeling. This method has been used for all test specimens, including those for the flexural test. The optimal parameters required for carrying out the test specimens through the printing process have been specified as infill density of 90%, thickness of top and bottom layers of 1mm, shell thickness of 0.4mm, speed of 5mm/s, and layer height of 0.1mm. Preliminary experiments and recommendations from published literature on FDM printing of PLA and PLA-based composites were taken into consideration when choosing the particular FDM processing parameters. In order to maximize load-bearing capacity and avoid the excessive thermal buildup associated with 100% infill, the 90% infill density was chosen to approximate near-solid conditions. Tab. 1 presents the composition of composite and corresponding fiber volume fractions for 3 wt% and 6 wt% CF/PLA composites. Increasing fiber loading from 3 wt% to 6 wt% increases the gross fiber volume fraction from 2.1 vol% to 4.3 vol%. When the 90% FDM infill density is considered, the effective fiber volume fraction slightly decreases to 1.9 vol% and 3.9 vol%, respectively. Flexural specimens have been specified and prepared based on the ASTM D790 standard. The ASTM D790 standard guarantees that bending strength of the material is properly tested, conforming to quality and specifications required. A simply supported specimen was loaded using a three-point loading system, and tests were performed using a universal tensile testing equipment with a crosshead speed of 3 mm/min.Fig.2 depicts the dimensions of the flexural test specimen.

In compliance with the ASTM D790 standard, which suggests testing with three specimens per condition to ensure statistical reliability, a minimum of three specimens were fabricated and tested under identical conditions for each material composition for neat PLA, PLA + 3 wt% CF, and PLA + 6 wt% CF. The average of these three tests is represented by the flexural strength values presented in the manuscript.

These standards are essential for accurate and repeatable measurements of flexural properties, and the specimens were meticulously prepared and tested to make sure they met them. [13]. Fig.3 presents the photograph of the FDM printed flexural test specimen. Fig.4 depicts the schematic of the flexural test as per ASTM standard.

Figure 2: Dimensions of the flexural test specimen.

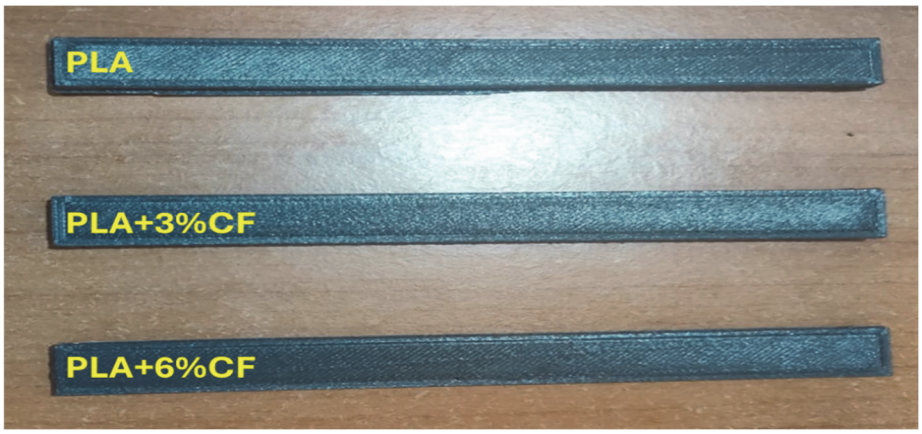

Figure 3: Photograph of FDM printed PLA and its composites.

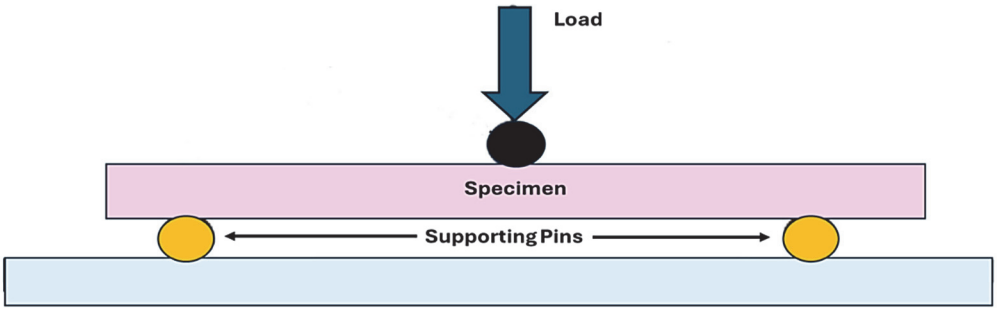

Figure 4: Schematic diagram of flexural test.

RESULTS AND DISCUSSION

Microstructure

Fig.5 depicts the microstructure of the extruded filament of PLA and PLA+CF composites. SEM was used to comprehensively examine the internal morphology of the PLA composite filament, both with and without short carbon fibers. Before the FDM printing process, the checks were made to assess the quality of the fiber-matrix bonding and confirm how evenly the fibers were distributed throughout the PLA matrix. At both reinforcing levels of 3% and 6%, scanning electron microscopy showed the uniform distribution of the short carbon fiber in the PLA matrix. The composite filaments showed no significant defects such as voids and fiber agglomerates, which indicates the acceptable integration of the reinforcement. Such consistent morphology and uniform fiber distribution play an important role in the achievement of predictable mechanical properties in the final FDM parts through effective load transfer and also ensure the overall structural integrity of the parts, which in turn directly leads to enhanced flexural performance. Moreover, the uniformity of carbon fibers is used to prevent crack propagation for improving the material with better resistance to failure under bending load. Such behavior is consistent with observations in other fiber reinforced composites showing that an increase in fiber content is generally associated with an increase in flexural strength [13]. However, this level of improvement is also related to the interfacial adhesion between the polymer matrices and the fibers since interfacial adhesion is an important parameter for efficient stress transfer. Intermittent failure may occur due to inadequate interfacial adhesion

between the fibers and the matrices as well as the presence of inter/intra fiber moisture, leading to decreased flexural strength as clarified by similar experiences with fiber-reinforced polymer composites.

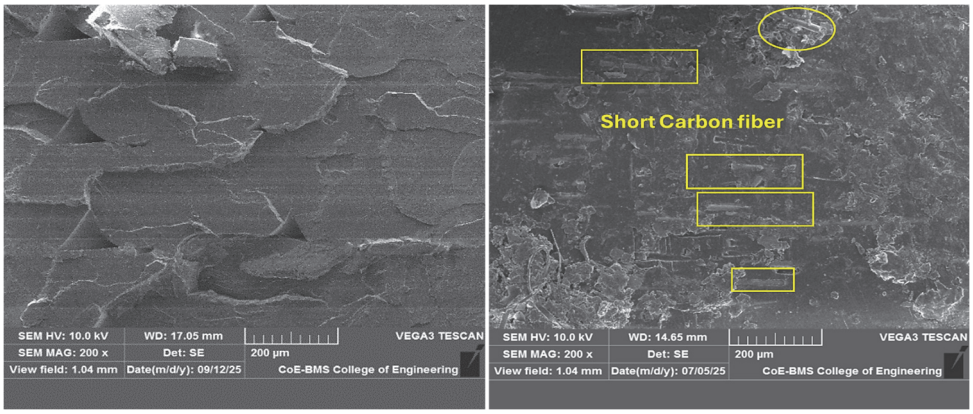

(a) PLA (b) PLA+3%CF

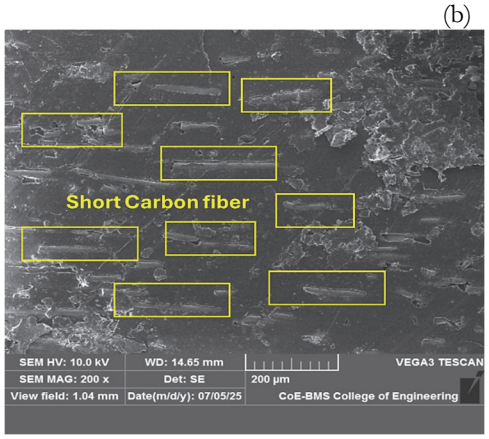

(c) PLA+6%CF

Figure 5: SEM images of extruded filaments depicting the carbon fibers dispersion

FLEXURAL STRENGTH

Figs. 6 and 7(a-b) present the stress-strain graph and graphical representation of flexural strength values and strain at failure of neat PLA and its carbon fiber-reinforced variants produced through FDM, and the overall pattern fairly shows a clear improvement trend. Flexural strength goes up as fiber content increases, showing the obvious trend. All values were derived from the three specimens per condition in line with ASTM D790 and presented in Fig. 7(a-b). Neat PLA exhibits 58 ± 3.2 MPa, which is the baseline everything else gets measured against. The stress strain curve for this material in Fig. 6 rises gradually through an elastic region and then transitions into a broader nonlinear zone before the specimen eventually fails at around 4.2 ± 0.3% strain. This response is obvious that one would expect from an unreinforced thermoplastic where the polymer chains are relatively free to move and the material can stretch a fair amount before failure. At 3 wt% carbon fiber, the average flexural strength was found to be 84 ± 4.1 MPa, and that is roughly 44.8% above neat PLA, which is a fairly substantial increase for a modest fiber addition. The fibers are likely taking on a proportionate share of the bending load and slowing down the possible damage process that would otherwise initiate earlier in the matrix [14, 15]. The elastic slope in Fig. 6 is noticeably steeper for this condition, which suggests the modulus has improved as well. Strain at failure has fallen to around 3.6 ± 0.2%, and this is probably because the fibers are physically getting in the way of chain segment movement, making the composite resistant to deform [14, 15].At 6 wt%, the strength reached 109 ± 5.6 MPa, which works out to nearly 87.9% above neat PLA and is the highest value recorded across all three conditions. The initial slope steepened again relative to both the unreinforced material and the 3 wt% composite, which is consistent with continued stiffness accumulation as more fiber is added. Strain at failure came down further to 2.9 ± 0.3%, and the pattern by this point is fairly clear in that more fiber means more constraint on the matrix and less capacity for deformation before fracture [14, 15].

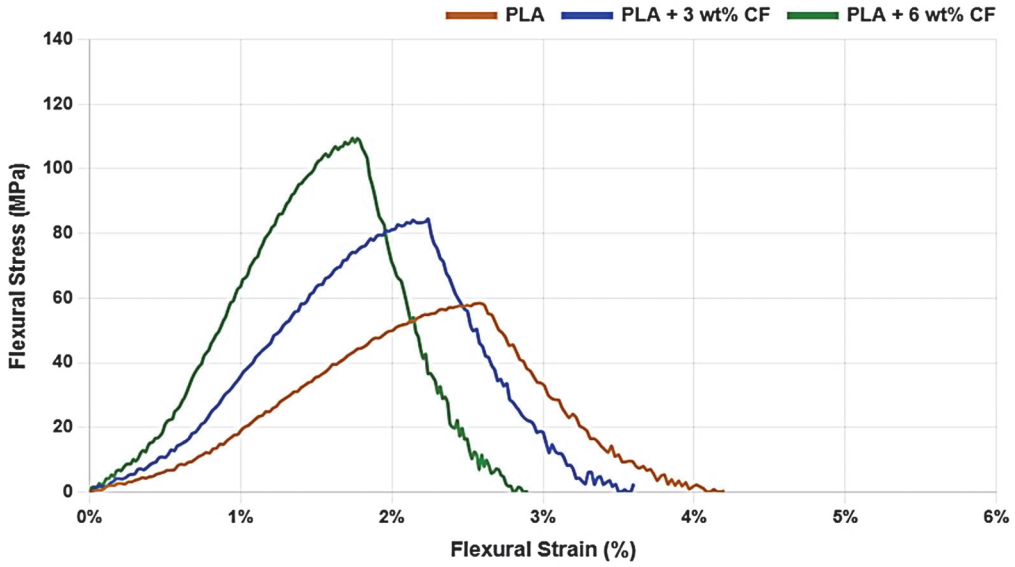

Figure 6: Flexural Stress-strain curve of FDM printed PLA and carbon fiber reinforced PLA composites

The mean flexural strength peaks at an individual value of 109 MPa for the composites containing 6 wt% carbon fiber, representing an overall improvement of about 88% compared to neat PLA. Correspondingly, the accompanying stress-strain curve displays the steepest slope among all tested samples, representing the maximum stiffness of the composite. This higher reinforcement level obviously converts into the lowest strain-to-failure of the same material, highlighting its increased brittleness with rising fiber content [16,17].

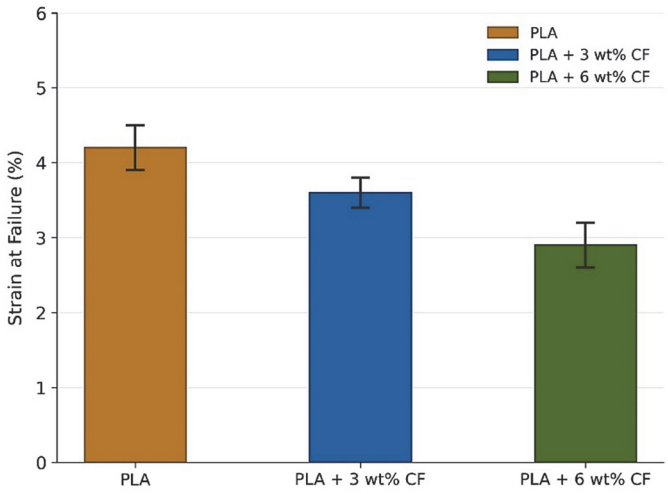

Figure 7a: Variation of flexural strength of PLA FDM printed PLA and carbon fiber reinforced PLA composites

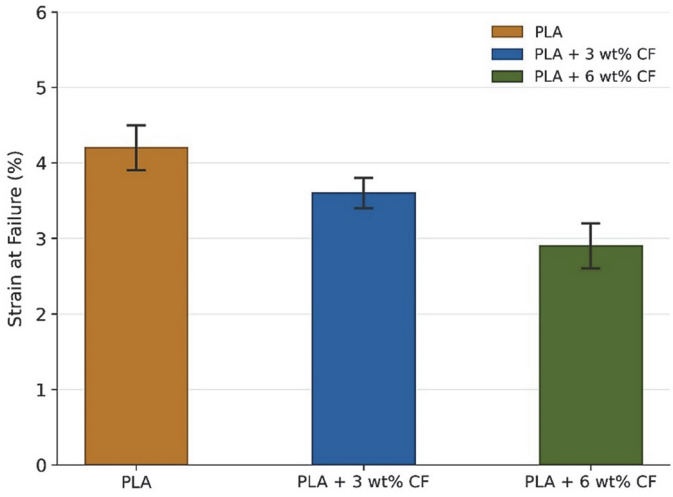

Figure 7b: Variation of strain at failure of PLA FDM printed PLA and carbon fiber reinforced PLA composites

The trends shown in Figs. 6 and 7(a-b) are discussed here. Short carbon fibers embedded in the PLA matrix take on a load-bearing role and redirect the applied bending stress away from the more compliant polymer toward the stiffer reinforcement, and that redistribution essentially leads to the strength gains observed across the two fiber contents tested. The 45% and 88% improvements at 3 wt% and 6 wt% CF, respectively, are consistent with this interpretation, and the scale of those gains arguably reflects the efficiency with which stress transfer was operating at the fiber-matrix interface under the specific FDM conditions used here. The 0.1 mm layer height and rectilinear infill at 90% density appear to have contributed to mechanical interlocking between the extruded PLA and the embedded fibers. SEM observations of fiber imprints and pull-out features on the fracture surfaces in Fig. 8 offer reasonably direct microstructural evidence that this interlocking was active during loading. Some shortfall relative to strength predictions is still expected given the layer-by-layer nature of FDM deposition and the likely presence of interlayer voids, though the reinforcement trend across both fiber contents remains fairly

unambiguous. Interestingly, the reduction in strain at failure is also worth addressing here. Rigid fiber inclusions constrain the mobility of PLA molecular chain segments, and as fiber content rises, this constraint intensifies, and the fracture behavior shifts progressively toward the brittle end of the spectrum [18, 19]. At 3 wt% CF, the material still retains enough ductility to be considered for semi-structural uses while delivering meaningfully better strength than neat PLA. At 6 wt%, the balance tips the other way, and stiffness, together with load-bearing capacity, becomes the dominant characteristic at the cost of deformation tolerance, which is broadly consistent with the literature reports for fiber-reinforced thermoplastics at comparable reinforcement levels [18, 19].

It has been confirmed that the short carbon fibers as an additive into PLA by means of FDM provides significant improvements in the flexural strength and stiffness although the ductility is reduced. From an engineering perspective, the observed percentage increases of about 45% for 3% CF and about 88% for 6% CF clearly prove the efficacy of carbon fibers as reinforcement agents. These results prove conclusively the appropriateness of carbon-fiber reinforced PLA composites with structural and functional demands manufactured by additive manufacturing, where outstanding mechanical performance is a critical attribute.

Prior work on FDM-printed CF/PLA systems has been discussed and compared here. Ning et al. [20] showed that flexural strength goes up as fiber content increases in PLA, though interfacial debonding and porosity at higher loadings tend to pull back some of that gain, and this is not entirely inconsistent with the 6 wt% CF results suggested in the present study. Tekinalp et al. [21] demonstrated that strain at failure drops when fibers are added and traced this back to the matrix being unable to deform freely around aligned fibers. The ductility falling from 4.2% down to 2.9% as recorded here follows more or less the similar pattern. On the other hand, raster orientation and its role in failure anisotropy are discussed by Parandoush and Lin [22] and worked through fairly carefully, and the fracture transition observed under SEM in this study moving from quasi-brittle toward semi-ductile sits reasonably well within that interpretation.

FLEXURAL FRACTURE SURFACE ANALYSIS

The investigation under a Scanning Electron Microscope on the fractured surface of flexural test samples offers critical information regarding the failure behavior of neat PLA, as well as short carbon fiber-reinforced PLA composites. The results observed under a scanning electron microscope at lower as well as higher magnifications confirm that morphological changes are directly related to stress/strain behavior, as observed in the corresponding flexural test results (Fig. 8).

The fractured surface of neat PLA is smooth by comparison and shows rather limited plastic deformation before the specimen ultimately fails. The fracture behavior of this material is predominantly the term "quasi-brittle. " Neat PLA recorded the highest strain at failure across all three conditions. The fracture morphology is perhaps better understood alongside the mechanical data in Fig. 6 rather than in isolation. The lowest flexural strength belongs to neat PLA, and this material outlasted both composites in terms of deformation before fracture, and that combination is worth stating clearly. The surface appearance is consistent with this interpretation even if the connection between morphology and ductility is not always immediately obvious from visual examination alone. From the close observations of the specimen, the river-like markings, together with mirror zones, are visible on the fracture surface. These features tend to indicate crack initiation at a fairly localized site followed by propagation that was relatively rapid given the limited resistance the unreinforced matrix could offer under flexural loading, and they sit reasonably well with the quasi-brittle characterization put forward above.

The brittle nature of failure is further supported by the observation of the fine striations and cleavage steps. Once the critical stress is reached, the absence of any secondary reinforcing phase leads to rapid fracture propagation and poor energy absorption. This explains the smooth plateau and abrupt drop in the stress–strain curve of PLA.[23, 24]

For 3% carbon fiber, the fractured surface shows a rougher morphology compared to neat PLA, with clear evidence of carbon fiber pull-out and fiber imprints within the PLA matrix. These features indicate that partial load transfer occurs between the fibers and the matrix, improving flexural strength relative to neat PLA. Fiber pull-out voids are distributed across the fracture plane, suggesting that interfacial adhesion is sufficient to contribute to improved stress transfer but not strong enough to completely prevent fiber debonding. The broken fiber ends and fiber–matrix debonding are evident. Microvoids surrounding the pulled-out fibers point to localized stress concentrations where crack propagation initiates.

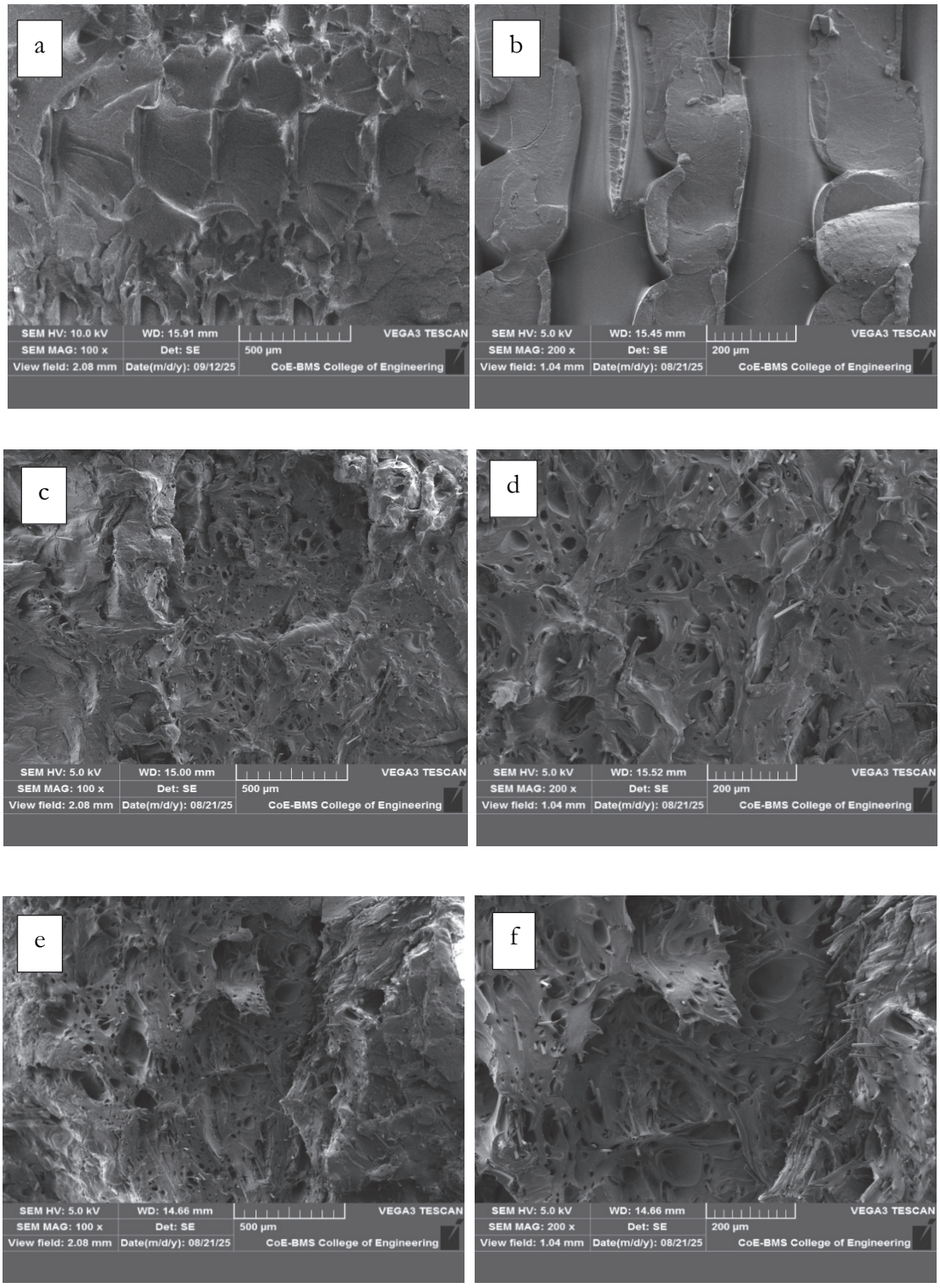

Figure 8: SEM images of flexural fractured surface of PLA (a-b) and CF reinforced PLA composites (b & c PLA+3%CF, e &f: PLA+6%CF).

Around the fiber sites, the matrix shows a measurable degree of plastic deformation, and this shifts the fracture character away from the quasi-brittle response seen in neat PLA toward something that sits closer to semi-ductile. The rougher morphology observed here correlates reasonably well with the stress-strain data, where the PLA + 3 wt% CF composite reaches 84 ± 4.1 MPa in flexural strength. Strain at failure does come down, though, from 4.2 ± 0.3% to 3.6 ± 0.2%, and that reduction is consistent with Fig. 6.For 6 wt% CF composite, the fracture surface becomes considerably rougher and

more tortuous than anything seen in either neat PLA or the 3 wt% material. Pulled-out fibers, fiber bridging, and fiber clusters are densely distributed across the surface. These features together suggest that the capacity of the composite to arrest crack advancement grows substantially as fiber content rises, and the outcome in terms of energy absorption and peak flexural strength at 109 ± 5.6 MPa is the best recorded across all three conditions evaluated in this study [25, 26].The fibers at this loading level appear more thoroughly anchored within the PLA matrix. Clean pull-out sites, which are visible in the 3 wt% composite, are comparatively rare here, and fibers are observed in a fractured condition, which implies the interfacial stress transfer was sufficient to load the fibers to failure rather than simply dislodge them. Hackle marks and localized deformation zones in the surrounding matrix further support the presence of an active stress redistribution mechanism during loading. Taken together these observations align broadly with the stress-strain response, where the 6 wt% CF composite sustains its load-bearing capacity across the full extent of its strain range before eventual fracture.

The SEM observations provide direct evidence on the mechanisms of strengthening that are present. Neat PLA fails due to brittle fracture which arises because of the lack of reinforcing fibers, resulting in a low energy dissipation. The 3% CF composite has an advantage of fiber pull out and partial load transfer, leading to an increase in strength and strain at failure. The 6% CF composite with higher reinforcement content shows the appearance of fiber fractures, fiber bridges, and more effective interfacial bonding, which are responsible for the highest flexural strength and better toughness. The progression of smooth fracture surfaces for neat PLA to more and more rough fiber dominated morphologies in the reinforced composites correlate well with the increasing stress-strain responses recorded during flexural testing. The formation process of the FDM itself is responsible for the formation of this fracture surface morphology. FDM's layer-by-layer deposition process may result in problems with interlayer adhesion and possible void creation, which may serve as places where cracks begin to spread. In the case of fiber reinforcement, these factors such as the alignment and distribution of the fibers that are set by the printing path and melt-pool characteristics of the FDM process also can control the way cracks propagate around or through the fibers which in turn controls the observed pullout, bridging and fracture behaviour [27, 28].

It is important to note that, during FDM extrusion the shear flow within the nozzle tends to push short carbon fibers toward the print direction, and orientation factors somewhere around 0.6 to 0.85 have been reported for such systems [20]. The converging geometry of the nozzle essentially forces the suspended fibers to rotate and settle along the extrusion axis before deposition even begins. When specimens are printed with a rectilinear raster running along the longitudinal axis, the fibers end up roughly coinciding with the direction where bending stress is highest [21]. Load transfer through shear lag and crack bridging is therefore reasonably efficient though perhaps not as ideal as the numbers might suggest. It is worth noting that this favorable orientation is a consequence of printing strategy rather than any intrinsic material behavior. At 3 wt% CF, the relatively sparse fiber population allows the flow field to orient fibers without much interference, and flexural gains follow accordingly. At 6 wt% CF, things become more complicated because fiber-to-fiber interactions grow more frequently, and agglomeration begins to erode the per-fiber contribution to stiffness and strength [22]. An 88% improvement in flexural strength was nonetheless recorded, which is a fairly substantial outcome. Perfect alignment is of course not achievable given that bead boundary constraints and nozzle wall effects and fiber breakage during extrusion all contribute to some degree of residual misorientation.

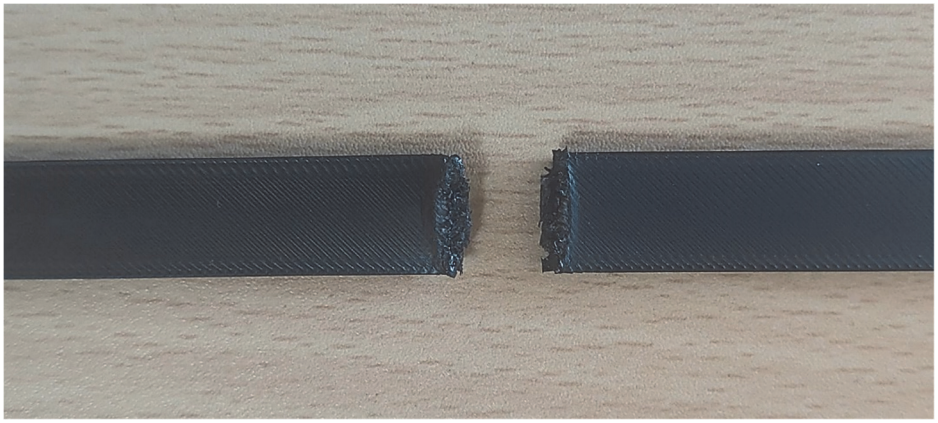

(a) PLA

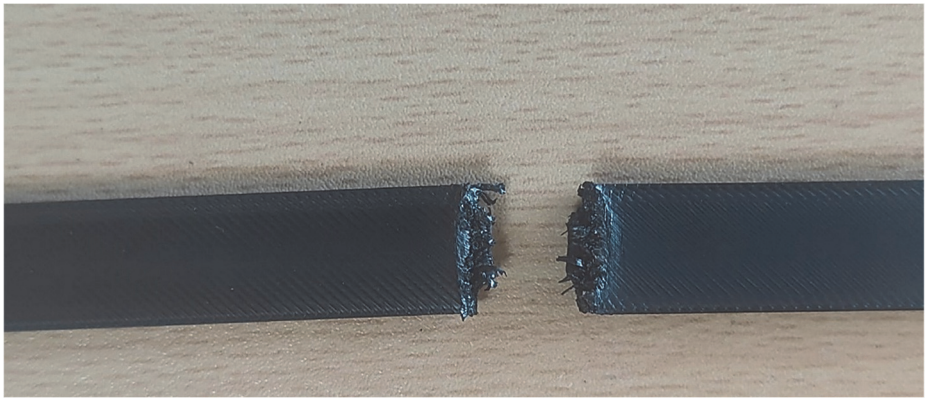

(b) PLA+3%CF

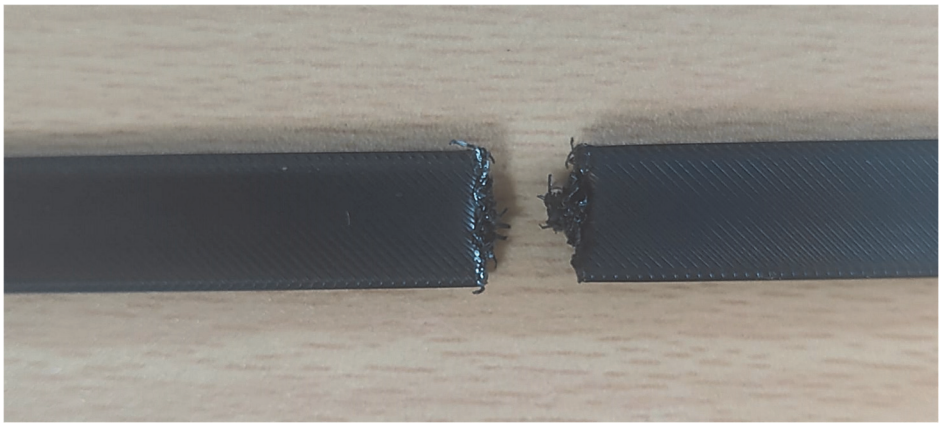

(c) PLA+6%CF

Figure 9: Photograph of the fractured specimens of the PLA and CF reinforced PLA composites

Fig. 9 depicts the photographs of the specimens captured after flexural tests. The captured fractured surface photographs corroborate the discussion above with reasonable consistency. In the neat PLA specimen, the smooth featureless surface visible in the image confirms the quasi-brittle fracture character described earlier and the absence of any fiber related features leaves little room for alternative interpretation. Moving to the 3 wt% CF specimen the photograph reveals scattered pull-out voids and visible fiber imprints across the fracture plane and the localized matrix deformation around these sites is discernible which supports the shift toward semi-ductile behavior and aligns with the recorded flexural strength and strain reduction. The 6 wt% CF fracture surfaces in the photograph appears markedly more tortuous and fiber dominated and fractured fiber ends rather than clean pull-out sites dominate the image confirming stronger interfacial stress transfer sufficient to fracture fibers rather than dislodge them and this is broadly consistent with the peak flexural strength. Taken together the photographic evidence and the SEM observations reinforce the progressive transition from brittle to toughened fracture behavior as fiber content increases from 0 to 6 wt% CF.

CONCLUSIONS

In conclusion, the thorough flexural analysis and in-depth fractographic analysis clearly show that the mechanical performance of FDM-fabricated PLA composites is much improved by the addition of short carbon fibers.

1. The use of short carbon fibers in PLA by FDM makes a significant enhancement in flexural strength and stiffness, which improved by about 45% for 3% CF and 88% for 6% CF compared to neat PLA, thus proving the effectiveness of carbon fiber as reinforcing agents.
2. A homogeneous dispersion of fibers without significant voids or agglomeration was found by SEM analysis of extruded filaments, ensuring dependable load transmission and predictable mechanical performance in the finished printed composites.

3. The fracture surface analysis showed that in reinforced composites, the morphologies changed from smooth and brittle in neat PLA to rougher and dominated by fibers. Features including fiber pull-out, fiber–matrix debonding, and fractured fibers were directly associated with higher strength and lower ductility.
4. Fiber fracture and bridging were more common at 6% CF, indicating better interfacial bonding but increased brittleness, whereas partial load transfer and fiber pull-out dominated at 3% CF, resulting in increased strength while preserving moderate ductility.
5. The fracture morphologies of FDM composites are affected by adhesiveness between layers and fiber orientation in FDM processing, and reinforcement helps prevent defects through deflection and stopping of fracture in FDM composites to increase their toughness and load capacity.

REFERENCES

[1] Somsuk, N., Pramoonmak, S., Chongkolnee, B., Tipboonsri, P. and Memon, A. (2025). Enhancing Mechanical Properties of 3D-Printed PLA Composites Reinforced with Natural Fibers: A Comparative Study, J. Compos. Sci., 9(4), p. 180. DOI: https://doi.org/10.3390/jcs9040180.

[2] Maqsood, N. and Rimašauskas, M. (2021). Characterization of Carbon Fiber Reinforced PLA Composites Manufactured by Fused Deposition Modeling, Compos. Part C Open Access, 4, p. 100112. DOI: https://doi.org/10.1016/j.jcomc.2021.100112.

[3] Alkabbanie, R., Aktaş, B., Demircan, G. and Yalçın, Ş.P. (2024). Short Carbon Fiber-Reinforced PLA Composites: Influence of 3D-Printing Parameters on the Mechanical and Structural Properties, Iran. Polym. J., 33(8), pp. 1065–1079. DOI: https://doi.org/10.1007/s13726-024-01315-8.

[4] Cao, M., Cui, T., Yue, Y., Li, C., Xue, G., Jia, X. et al. (2022). Investigation of Carbon Fiber on the Tensile Property of FDM-Produced PLA Specimen, Polymers, 14(23), p. 5230. DOI: https://doi.org/10.3390/polym14235230.

[5] Elfaleh, I., Abbassi, F., Habibi, M., Ahmad, F., Guedri, M., Nasri, M. et al. (2023). A Comprehensive Review of Natural Fibers and Their Composites: An Eco-Friendly Alternative to Conventional Materials, Results Eng., 19, p. 101271. DOI: https://doi.org/10.1016/j.rineng.2023.101271.

[6] Siddalingappa, S., Pal, B., Haseebuddin, M.R. and Gopalakrishna, K. (2020). Tribological Behaviour of Carbon Fibre Polymer Composites Reinforced with Nano-fillers, In: Lecture Notes in Mechanical Engineering, Singapore, Springer Nature, p. 791. DOI: https://doi.org/10.1007/978-981-15-1201-8_84.

[7] Ferreira, R.T.L., Amatte, I.C., Dutra, T.A. and Bürger, D. (2017). Experimental Characterization and Micrography of 3D Printed PLA and PLA Reinforced with Short Carbon Fibers, Compos. Part B Eng., 124, pp. 88–100. DOI: https://doi.org/10.1016/j.compositesb.2017.05.013.

[8] Sanei, S.H.R. and Popescu, D. (2020). 3D-Printed Carbon Fiber Reinforced Polymer Composites: A Systematic Review, J. Compos. Sci., 4(3), p. 98. DOI: https://doi.org/10.3390/jcs4030098.

[9] Dickson, A., Abourayana, H.M. and Dowling, D.P. (2020). 3D Printing of Fibre-Reinforced Thermoplastic Composites Using Fused Filament Fabrication — A Review, Polymers, 12(10), p. 2188. DOI: https://doi.org/10.3390/polym12102188.

[10] Pervaiz, S., Qureshi, T.A., Kashwani, G. and Kannan, S. (2021). 3D Printing of Fiber-Reinforced Plastic Composites Using Fused Deposition Modeling: A Status Review, Materials, 14(16), p. 4520. DOI: https://doi.org/10.3390/ma14164520.

[11] Yang, Y., Yang, B., Chang, Z., Duan, J. and Chen, W. (2023). Research Status of and Prospects for 3D Printing for Continuous Fiber-Reinforced Thermoplastic Composites, Polymers, 15(17), p. 3653. DOI: https://doi.org/10.3390/polym15173653.

[12] Marabello, G., Borsellino, C. and Bella, G.D. (2023). Carbon Fiber 3D Printing: Technologies and Performance — A Brief Review, Materials, 16(23), p. 7311. DOI: https://doi.org/10.3390/ma16237311.

[13] Haseebuddin, M.R., Lobo, A., Das, A.N.M., Harsha, S.P., Acharya, K.G. and Balaji, G. (2024). Effect of Aging on Flexural Behavior of Disposed Glass Fiber Reinforced Bamboo Mat–Polyester Composites, J. Inst. Eng. (India) Ser. D, Online First. DOI: https://doi.org/10.1007/s40033-024-00676-x.

[14] Valente, B.F.A., Silvestre, A.J.D., Neto, C.P., Vilela, C. and Freire, C.S.R. (2022). Improving the Processability and Performance of Micronized Fiber-Reinforced Green Composites through the Use of Biobased Additives, Polymers, 14(17), p. 3451. DOI: https://doi.org/10.3390/polym14173451.

[15] Wang, H., Hassan, E.A.M., Memon, H., Elagib, T.H.H. and AllaIdris, F.A. (2019). Characterization of Natural Composites Fabricated from Abutilon-Fiber-Reinforced Poly(Lactic Acid), Processes, 7(9), p. 583. DOI: https://doi.org/10.3390/pr7090583.

[16] Lin, J.H., Huang, C.L., Chen, C.K., Liao, J.M. and Lou, C.W. (2015). Manufacturing and Mechanical Property Evaluations of PLA/Carbon Fiber/Glass Fiber Composites, Appl. Mech. Mater., 749, pp. 261–264. DOI: https://doi.org/10.4028/www.scientific.net/AMM.749.261.

[17] Ismail, K.I., Yap, T.C. and Ahmed, R. (2022). 3D-Printed Fiber-Reinforced Polymer Composites by Fused Deposition Modelling (FDM): Fiber Length and Fiber Implementation Techniques, Polymers, 14(21), p. 4659. DOI: https://doi.org/10.3390/polym14214659.

[18] Karimi, A., Rahmatabadi, D. and Baghani, M. (2024). Various FDM Mechanisms Used in the Fabrication of Continuous-Fiber Reinforced Composites: A Review, Polymers, 16(6), p. 831. DOI: https://doi.org/10.3390/polym16060831.

[19] Beckman, I.P., Lozano, C., Freeman, E. and Riveros, G.A. (2021). Fiber Selection for Reinforced Additive Manufacturing, Polymers, 13(14), p. 2231. DOI: https://doi.org/10.3390/polym13142231.

[20] Parandoush, P. and Lin, D. (2017). A Review on Additive Manufacturing of Polymer-Fiber Composites, Compos. Struct., 182, pp. 36–53. DOI: https://doi.org/10.1016/j.compstruct.2017.08.088.

[21] Ning, F., Cong, W., Qiu, J., Wei, J. and Wang, S. (2015). Additive Manufacturing of Carbon Fiber Reinforced Thermoplastic Composites Using Fused Deposition Modeling, Compos. Part B Eng., 80, pp. 369–378. DOI: https://doi.org/10.1016/j.compositesb.2015.06.013.

[22] Tekinalp, H.L., Kunc, V., Velez-Garcia, G.M., Duty, C.E., Love, L.J., Naskar, A.K. et al. (2014). Highly Oriented Carbon Fiber–Polymer Composites via Additive Manufacturing, Compos. Sci. Technol., 105, pp. 144–150. DOI: https://doi.org/10.1016/j.compscitech.2014.10.009.

[23] Ahmed, H.A., Hussain, G., Gohar, S., Ali, A. and Alkahtani, M. (2021). Impact Toughness of Hybrid Carbon Fiber-PLA/ABS Laminar Composite Produced through Fused Filament Fabrication, Polymers, 13(18), p. 3057. DOI: https://doi.org/10.3390/polym13183057.

[24] Pan, Y., Lin, Z.I., Lou, C., Huang, C., Lee, M.C., Liao, J.M. et al. (2018). Polylactic Acid/Carbon Fiber Composites: Effects of Polylactic Acid-g-Maleic Anhydride on Mechanical Properties, Thermal Behavior, Surface Compatibility, and Electrical Characteristics, J. Compos. Mater., 52(3), pp. 405–416. DOI: https://doi.org/10.1177/0021998317708020.

[25] Lee, J.H., Park, C.G. and Kim, S.H. (2023). Impact Fracture Mechanism and Heat Deflection Temperature of PLA/PEICT Blends Reinforced by Glass Fiber, RSC Adv., 13(32), pp. 22315–22324. DOI: https://doi.org/10.1039/d3ra03692h.

[26] Prajapati, A.R., Dave, H.K. and Raval, H.K. (2021). Effect of Fiber Reinforcement on the Open Hole Tensile Strength of 3D Printed Composites, Mater. Today Proc., 46, pp. 8629–8635. DOI: https://doi.org/10.1016/j.matpr.2021.03.597.

[27] Albadrani, M.A. (2022). Failure Prediction in 3D Printed Kevlar/Glass Fiber-Reinforced Nylon Structures with a Hole and Different Fiber Orientations, Polymers, 14(20), p. 4464. DOI: https://doi.org/10.3390/polym14204464.

[28] Sharafi, S., Santare, M.H., Gerdes, J. and Advani, S.G. (2021). A Review of Factors that Influence the Fracture Toughness of Extrusion-Based Additively Manufactured Polymer and Polymer Composites, Addit. Manuf., 38, p. 101830. DOI: https://doi.org/10.1016/j.addma.2020.101830.